CrystEngComm

RSC Publishing

COMMUNICATION

View Article Online
View Journal | View Issue

Photoluminescence of core–shell nanoparticles made from yttrium stabilized zirconia powder grain coated with alumina

Cite this: *CrystEngComm*, 2013, **15**, 3292

Received 20th December 2012,
Accepted 28th February 2013

DOI: 10.1039/c3ce27071h

www.rsc.org/crystengcomm

Rosana F. Gonçalves,[a] José T. O. Figueiredo,[a] Alberthmeiry T. de Figueiredo,*[a] Maximo Siu Li,[b] Elson Longo[c] and Mario J. Godinho[a]

A YSZ@Al_2O_3 nanocomposite was obtained by Al_2O_3 coating on the surface of yttrium stabilized zirconia *via* a polymeric precursor method. The resulting core–shell structures were characterized by X-ray diffraction, scanning electron microscopy, transmission electronic microscopy and PL spectra. The TEM micrographs clearly show a homogeneous Al_2O_3 shell around the ZrO_2 core. The observed PL is related to surface–interface defects. Such novel technologies can, in principle, explore materials which are not available in the bulk single crystal form but their figure-of-merit is dramatically dependent on the surface–interface defect states.

1 Introduction

Nanocomposite ceramics have received significant scientific and technological attention over the past several decades. Nanocoated particles are an entirely new class of materials, manifesting considerable potential for new applications.[1–6] The combination of two materials on a nanometer scale, one acting as a core and the other as a coating, can result in interesting physical and chemical properties that are substantially different from those of the core, thus making them attractive from both a scientific and technological viewpoint.[7,8] The growth defects and stress, resulting in the formation of locally coherent interfaces, are the most important factors responsible for an increase in the coating strength.[9] For instance, Brovelli *et al.*[10] identified radiative and non-radiative decay rates in interface defects and they quantified the energy transfer process in the erbium doped SnO_2:SiO_2 system.

Special interest is currently being granted to the YSZ@Al_2O_3 system because it is hard to dissolve one component into the other in a solid solution. This is favorable to inhibit grain growth primarily by the interdiffusion of atoms along the relevant grain and interphase boundaries in a controlled composite microstructure.[7]

Photoluminescence (PL) spectroscopy is one of the most powerful methods for studying the structural order–disorder effects in materials and is a quantum phenomenon. To observe PL emissions, certain defects should be present in the network material.[11–14] Studies of ZrO_2 and yttrium stabilized ZrO_2 nanocrystals luminescence as well as yttrium stabilized single crystal luminescence and induced absorption have shown that in the material the intrinsic defects are responsible for their luminescence at room temperature.[15] In addition, surface modification of a wide band gap semiconducting shell around a narrow band gap core can alter the charge, functionality and reactivity of the materials and consequently enhance the functional properties due to localization of the electron–hole pairs.[16–19] In addition, Rauback *et al.*[20] reported the photoluminescence emission of core–shell Al_2O_3@ZrO_2 and they correlated the interfacial structure and optical features.

The aim of the present work is to correlate the presence of surface–interface defects and the luminescence property with a nanocomposite ceramic made from yttrium stabilized zirconia powder grains coated with alumina.

2 Experimental

The start materials were aluminium nitrate, (Aldrich, purity > 99.9%) high purity Yttria-stabilized zirconia (Tosoh grade YSZ, purity > 99.9%), citric acid (E. Merck, purity > 99.9%) and ethylene glycol (Mallinckrodt Baker). The synthetic route was similar to Raubac *et al.*[20] The crystalline commercial YSZ powder was dispersed in water using an ultra-sonic probe. An aluminium polymeric precursor water-based solution, aluminium citrate, was used to coat the YSZ nanocrystals. The aluminium citrate aqueous solution was prepared from aluminium nitrate and citric acid. Ethylene glycol was added to the citric acid to promote a polymerization reaction. The molar relations were 1 : 3 : 2 of citric acid, aluminium and ethylene glycol, respectively. This Al solution was added to the ZrO_2 aqueous suspension (relation molar, xAl/Zr, where x = 1, 3 and 5%) and then the solvent was evaporated at 70 °C with a rotary evaporator. The dried material was heat treated for 4 h at 350 °C to remove the organic waste.[7]

[a]*Department of Chemistry – CAC/UFG, 75.704-020, Catalão, GO, Brazil. E-mail: alberthmeiry.figueiredo@catalao.ufg.br*
[b]*Institute of Phisics, 13.566-590, USP-São Carlos, SP, Brazil*
[c]*INCTMN, Institute of Chemistry UNESP, 14.801-970, Araraquara, SP, Brazil*

The final composition of YSZ@XAl$_2$O$_3$ has X = 1, 3 and 5 mol% zirconia. The YSZ@XAl$_2$O$_3$ was heat treated at 400, 500 and 600 °C for 2 hours using a heating rate of 5 °C min^{-1}.

The obtained powders were structurally characterized by X-ray diffraction (XRD) collected from 5 to 75° in the 2θ range using Cu–Kα radiation (Rigaku-DMax/2500PC). The coated powders were observed with the use of a transmission electron microscope (TEM) using a JEOL 3010 ARP microscope operating at an acceleration voltage of 300 kV. PL spectra were collected with a Thermal Jarrel-Ash Monospec monochromator and a Hamamatsu R446 Photomultiplier. The 350.7 nm (2.57 eV) exciting wavelength of a krypton ion laser (Coherent Innova) was used with the output of the laser kept at 200 mW. All measurements were taken at room temperature.

3 Results and discussion

Fig. 1a presents X-ray diffractograms of the YSZ@XAl$_2$O$_3$ (X = 5%). Only the diffractions peaks of YSZ can be identified because the Al precursor concentration is too low for XRD analysis. YSZ was completely indexed in the tetragonal phase from JCPDS 38-1437. The same behavior was observed for YSZ@XAl$_2$O$_3$ (X = 1 and 3%). In order to verify the structural Al order–disorder, heat treatment of the aluminum precursor resin was made at 400 and 1100 °C (Fig. 1b).

The structurally ordered powder obtained by heat treatment at 1100 °C presents only diffractions peaks of single phase of Al$_2$O$_3$ and could be completely indexed on the basis of α-Al$_2$O$_3$ (JCPDS 05-0712). On the order hand, the XRD patterns of the powders annealed at 400 °C did not show any diffraction peaks, indicating that these materials are structurally disordered.

Though the alumina presence can not be detected by XRD analysis, the presence of coating in the samples can be confirmed by TEM micrographs (Fig. 2).

The TEM micrographs of the coated YSZ@XAl$_2$O$_3$ (X = 5%) heat treated at 400 °C reveal almost spherical particles which consist of a core of YSZ surrounded by a coating of alumina. The core is structurally ordered, whereas the coating is structurally disordered. Fig. 2a and 2b confirm that the Al$_2$O$_3$ forms a nanoshell over the YSZ core. Fig. 2c shows the EDX analysis of this sample. It can confirm the presence of aluminium in the sample.

When a nanoshell of structurally disordered Al$_2$O$_3$ is coated into structurally ordered YSZ, the core–shell result presents structural disorder at the junction of the materials. The structural disorder of the Al$_2$O$_3$ shell contributes to increase structural disorder in the material. In the literature, there are several papers explaining the favorable conditions for PL emission in materials presenting a certain structural order–disorder degree. The surface modification of a wide band gap semiconducting shell around a narrow band gap core can alter the charge, functionality and reactivity of the materials and consequently enhance the functional properties due to localization of the electron–hole pairs.[19,21,22]

The PL spectrum of the structurally ordered YSZ and structurally disordered Al$_2$O$_3$ and YSZ@XAl$_2$O$_3$ (X = 5%) samples are shown in Fig. 3. The structurally ordered YSZ and structurally

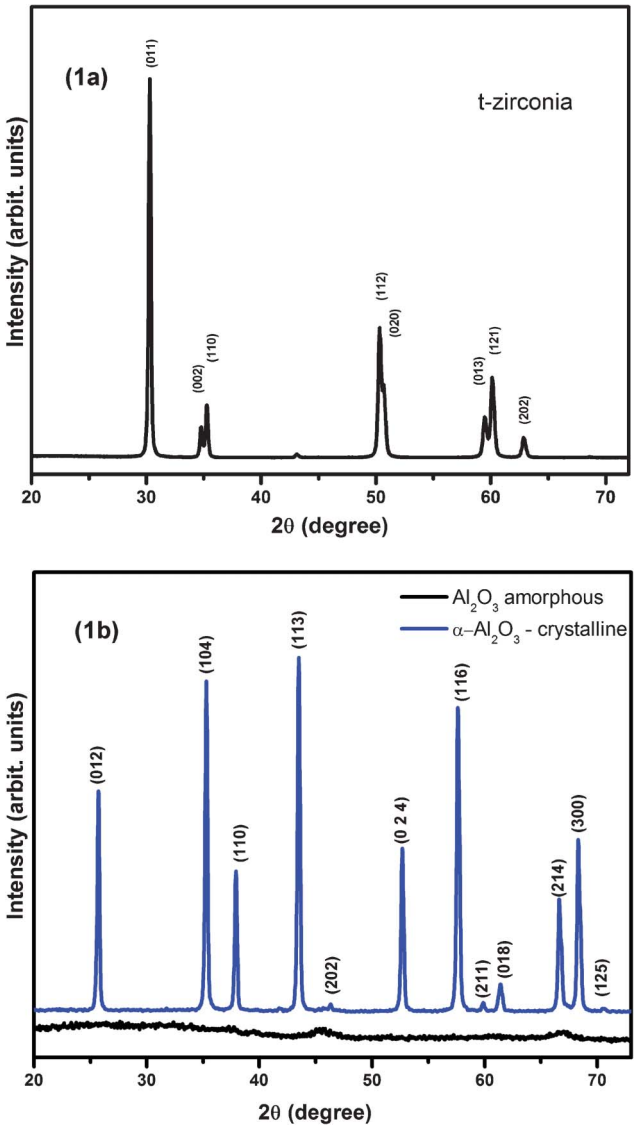

Fig. 1 X-ray patterns of: (a) YSZ@Al$_2$O$_3$ and (b) Al$_2$O$_3$ heat treatment at 400 and 1100 °C.

disordered Al$_2$O$_3$ present low PL intensities, in agreement with the literature. However, the YSZ@Al$_2$O$_3$ core shell presents high PL emission. PL is directly associated with the structural order–disorder. The first layers of Al$_2$O$_3$ tend to organize in the unit cell of the core (YSZ). However, the layers after the interface tend to deposit in the structure of alumina.[23] The structural disorder is high because competition occurs at the interface between the structure of zirconia and the alumina structure. Breaking the symmetry processes of these structures, such as distortions, breathings and tilts, creates a huge number of different structures and subsequently, different materials properties and this phenomenon can be related to local (short), intermediate and long-range structural order–disorder.[24] Such conditions are essential to the PL emission of YSZ@Al$_2$O$_3$.

A general aspect of the spectra is a broad band covering a large part of the visible spectra from ~370 to 750 nm. The line shape is

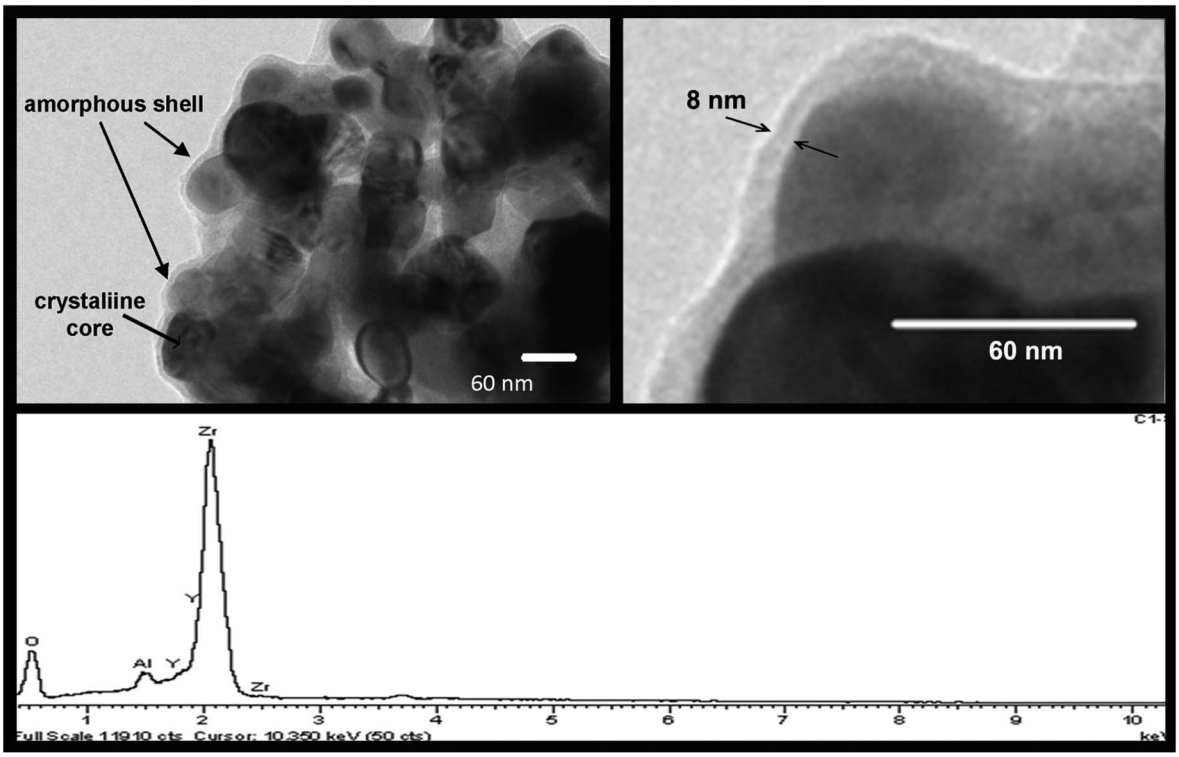

Fig. 2 TEM micrographs of YSZ@Al_2O_3 heat treated at 400 °C.

typical of the multiphonon process, *i.e.*, it has several relaxation channels, which are indicative of the presence of structural defects. Fig. 4 shows the relationship between the PL emission of YSZ@Al_2O_3 and the amount of Al_2O_3 coating. This graph shows that with an increase in the amount of Al_2O_3 coating, the PL intensity and the maximum of the PL intensity increases. The intensity of the PL emission increases because better coating and more bonds between YSZ and Al_2O_3 occurs. The structural disorder of the Al_2O_3 nanoshell allows several relaxation channels, which are indicative of delocalized levels. Thus, the maximum of the PL emission band shifts to a higher wavelength.

In order to evaluate the effect of the structural disorder in the Al_2O_3 nanoshell, YSZ@Al_2O_3 was heat treated at different temperatures. The disordered Al_2O_3 nanoshell becomes more structurally ordered with increased annealing times. This structural change also alters the electronic levels in the band gap. Fig. 4

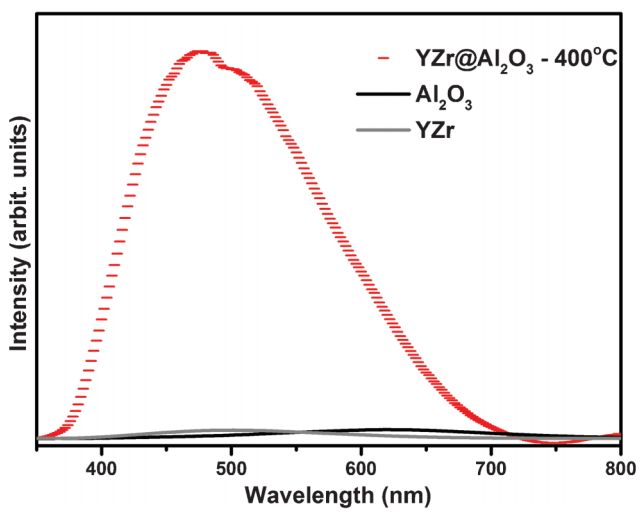

Fig. 3 PL spectra of structurally ordered YSZ and structurally disordered Al_2O_3 and YSZ@Al_2O_3.

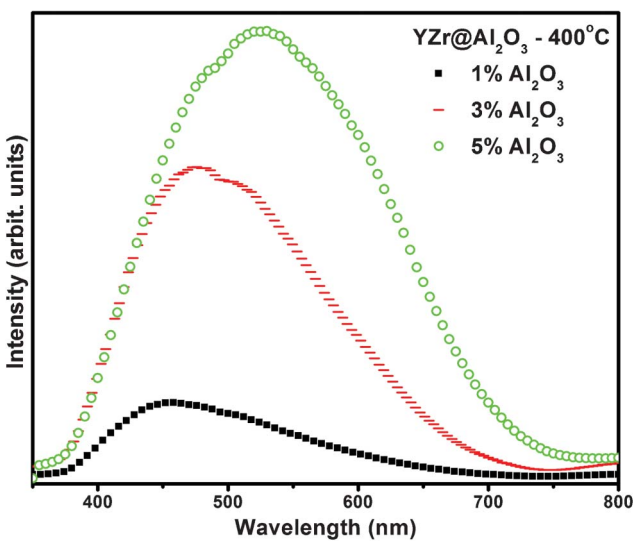

Fig. 4 PL spectra of YSZ@$X$$Al_2O_3$, with X = 1, 3 and 5%.

illustrates that the PL emission reduces with an increase of the Al_2O_3 amount. The PL emission is related to the structural order–disorder and in a structurally disordered solid, there is no complete order of atomic positions. The aforementioned experimental results strongly indicate that photoluminescence is directly related to the structural disorder in the interface.

4 Conclusions

It was possible to conclude that an interesting system was prepared by a soft method and presents nanoshells of Al_2O_3 over a YSZ core, *i.e.*, disordered alumina layers are the shell and the polycrystalline YSZ is the core. YSZ or Al_2O_3 alone do not show PL emission, however, the nanocomposite YSZ@Al_2O_3 presents a high broad band PL emission linked to the structural order–disorder. The surface–interface defect states are the main defects in the system. In addition, the nanoshell presents high structural disorder.

Acknowledgements

The authors thank the Brazilian research financing institutions FAPEG, CNPq, CNPq/INCTMN and CAPES for their funding of this work.

References

1 C. Y. Li, C. Ma, F. Wang, Z. J. Xi, Z. F. Wang, Y. Deng and N. Y. He, *J. Nanosci. Nanotechnol.*, 2012, **12**, 2964.
2 R. G. Chaudhuri and S. Paria, *Chem. Rev.*, 2012, **112**, 2373.
3 S. Y. Wei, Q. Wang, J. H. Zhu, L. Y. Sun, H. F. Lin and Z. H. Guo, *Nanoscale*, 2011, **3**, 4474.
4 W. Schartl, *Nanoscale*, 2010, **2**, 829.
5 P. Reiss, M. Protiere and L. Li, *Small*, 2009, **5**, 154.
6 J. R. Chen and J. Hu, *Aust. J. Chem.*, 2009, **62**, 1561.
7 R. F. Goncalves, M. J. Godinho, E. R. Leite, A. P. Maciel, E. Longo and J. A. Varela, *J. Mater. Sci.*, 2007, **42**, 2222.
8 C. J. Dalmaschio, V. R. Mastelaro, P. Nascente, J. Bettini, J. L. Zotin, E. Longo and E. R. Leite, *J. Colloid Interface Sci.*, 2010, **343**, 256.
9 L. Major, W. Tirry and G. Van Tendeloo, *Surf. Coat. Technol.*, 2008, **202**, 6075.
10 S. Brovelli, N. Chiodini, A. Lauria, F. Meinardi and A. Paleari, *Solid State Commun.*, 2006, **138**, 574.
11 M. L. Moreira, P. G. C. Buzolin, V. M. Longo, N. H. Nicoleti, J. R. Sambrano, M. S. Li, J. A. Varela and E. Longo, *J. Phys. Chem. A*, 2011, **115**, 4482.
12 L. S. Cavalcante, M. F. C. Gurgel, A. Z. Simoes, E. Longo, J. A. Varela, M. R. Joya and P. S. Pizani, *Appl. Phys. Lett.*, 2007, **90.**
13 L. Gracia, V. M. Longo, L. S. Cavalcante, A. Beltran, W. Avansi, M. S. Li, V. R. Mastelaro, J. A. Varela, E. Longo and J. Andres, *J. Appl. Phys.*, 2011, **110.**
14 M. L. Moreira, J. Andres, V. M. Longo, M. S. Li, J. A. Varela and E. Longo, *Chem. Phys. Lett.*, 2009, **473**, 293.
15 K. Smits, L. Grigorjeva, D. Millers, A. Sarakovskis, J. Grabis and W. Lojkowski, *J. Lumin.*, 2011, **131**, 2058.
16 M. J. L. Santos, J. Ferreira, E. Radovanovic, R. Romano, O. L. Alves and E. M. Girotto, *Thin Solid Films*, 2009, **517**, 5523.
17 L. Wang, H. W. Wei, Y. J. Fan, X. Z. Liu and J. H. Zhan, *Nanoscale Res. Lett.*, 2009, **4**, 558.
18 A. Ishizumi and Y. Kanemitsu, *Adv. Mater.*, 2006, **18**, 1083.
19 R. G. Xie, U. Kolb, J. X. Li, T. Basche and A. Mews, *J. Am. Chem. Soc.*, 2005, **127**, 7480.
20 C. W. Raubach, M. Z. Krolow, M. F. Mesko, S. Cava, M. L. Moreira, E. Longo and N. L. V. Carreno, *CrystEngComm*, 2012, **14**, 393.
21 J. F. A. Oliveira, T. M. Milao, V. D. Araujo, M. L. Moreira, E. Longo and M. I. B. Bernardi, *J. Alloys Compd.*, 2011, **509**, 6880.
22 M. A. Malik, P. O'Brien and N. Revaprasadu, *Chem. Mater.*, 2002, **14**, 2004.
23 W. D. Callister, in *Material Science and Engineering: An Introduction*, John Wiley & Sons, New York, 2007, pp. 721.
24 V. M. Longo, L. S. Cavalcante, E. C. Paris, J. C. Sczancoski, P. S. Pizani, M. S. Li, J. Andres, E. Longo and J. A. Varela, *J. Phys. Chem. C*, 2011, **115**, 5207.